Clocks and Accelerometers for Space Tests of Fundamental Physics

Lute Maleki, James M. Kohel, Nathan E. Lundblad, John D. Prestage, Robert J. Thompson, and Nan Yu

Quantum Sciences and Technology Group Jet Propulsion Laboratory, California Institute of Technology Pasadena, California, USA
lute.maleki@jpl.nasa.gov

Summary. In this chapter we discuss a technology development program at JPL to address the diminished opportunities for experimental tests of fundamental physics in space. By developing instruments that can serve multiple functions, we hope to gain flight opportunities that would otherwise be unavailable, due to recent refocusing of the space science mission in support of manned flights. We discuss the development of a liter-sized clock based on trapped mercury ions that can serve one-way navigation functions, as well as provide high stability for sensitive tests of general relativity, and possible variation of fine structure constant. We also describe progress in the development of an atom interferometer-based gravity gradiometer. This instrument is aimed at providing detailed subsurface mapping of earth and planetary bodies. It can also be used, with minor modifications, to serve as an instrument to test the equivalence principle. Finally, we report on recent progress for the development of a dual-beam atom laser based on spinor condensates, for future advanced instrumentation supporting fundamental physics studies in space.

1 Introduction

Since the early days of space exploration, the value of laboratory style experiments with clocks and accelerometers in space to test the fundamental models of physics has been well recognized. These "laboratory instruments" were identified as effective tools to test the range of validity of general relativity (GR), and soon missions such as Gravity Probe A and B were designed. It is noteworthy, however, that NASA did not select a follow-on mission to Gravity Probe A, which consisted of a hydrogen maser clock onboard a Scout rocket in a suborbital flight in 1976, until the mid-1990s. This is because tests of fundamental physics did not constitute a priority for space investigations, which mostly concentrated on observational investigations of the solar system and the space beyond.

In the 1990s two sets of unrelated developments rekindled the interest in testing physics with laboratory style experiments in space. On the theoretical

front, the physics community had reached the consensus that the Standard Model fell short of providing a complete picture of the physical universe. The proper theory that would adequately address unanswered questions such as the link between gravity and quantum fields is likely to be based on radically new schemes such as M theory. This view has been reenforced by the observational astronomy that has radically changed our view of the evolution of the universe, leading to a nearly complete reformulation of cosmology. We now generally believe that our universe is flat, and is expanding at an accelerated rate. These discoveries, together with the previously known inadequacies related to, for example, the physics of black holes further amplify the need for a new physical model that can adequately describe the underlying basis for astronomical observations.

The second development pertained to the interest in conducting fundamental science on the International Space Station (ISS). The ISS was designed as a platform to conduct microgravity science, and it was apparently very well suited for laboratory style instruments as well. The use of clocks and accelerometers to test fundamental physics, then, was a natural step in the utilization of scientific potential of the ISS, especially since these instruments could indeed benefit from the microgravity environment to enhance their sensitivity. Soon, the ESA and NASA planned several clock and accelerometer experiments with instruments that were based on new technologies fueled by laser cooling of atoms, and atom wave interferometry. These planned investigations in turn spurred new interest in the physics community, and several new experiments to test GR and look for possible variation of fundamental constants were proposed. These proposals, several of which are described in this volume, are based on platforms other than the ISS, and continue to be under study today.

Despite these renewed interest, the prospects for missions based on instruments such as clocks and accelerometers are realistically rather poor. This is because of the recent plans to limit the utilization of the ISS, and focus the bulk of space missions to explore Moon and Mars. The challenge presented by sustaining the ISS for the next few years, and developing the infrastructure for manned missions to the moon within a fixed budget, has placed severe constraints on the NASA budget, with a correspondingly similar situation for ESA.

With this backdrop, the focus of fundamental physics research at the Quantum Sciences and Technology Group at JPL has been reformulated. Realizing that independent missions such as spacetime [1], and ISS investigations such as PARCS and QuITE are not realistically viable in the current budget environment of NASA, which is likely to remain constrained in the next several years, we have shifted our focus toward the development of science experiments that can be performed as adjunct to other space missions. In particular, we have focused on the development of technologies that reduce size, cost, and power of precision instruments, allowing them to become attractive for applications other than tests of fundamental physics. By designing

and developing instruments that can satisfy needed functions in completely different areas of space exploration, such as navigation and subsurface mapping, we hope to create more opportunity for tests of fundamental physics.

In the following sections, we provide brief descriptions of the development of a small high performance clock with 1 l of volume and about 1 kg of mass, and an atom wave interferometer for gravity gradiometry. We will also give a short description of experiments toward more advanced accelerometers based on Bose–Einstein condensation.

2 LITE: A Liter-Sized High Performance Atomic Clock

The development of high performance atomic clocks based on ion traps is motivated by the inherent immunity of trapped ions to perturbing influences on the atomic energy structure, which in turn influence the stability of the clock. Ions in a trap do not experience collisions with the walls of a container, or with themselves. The use of heavier ions, such as mercury, allows lowering the sensitivity of the clock transition to the perturbing magnetic fields. These and other similar attributes of ion traps have led to the development of clocks that use microwave or optical transitions in a variety of ion systems.

At JPL, the work in the past two decades has been the development of a stable clock based on trapped mercury ion with performance parameters, including operational reliability, superior to that of the hydrogen maser, which has been the workhorse of navigation and communications system at NASA's deep-space network (DSN). After a successful demonstration of such an instrument dubbed the Linear Ion Trap Standard (LITS) based on mercury ions, the focus of the work has been placed on the development of a small, high performance clock suitable for direct deployment onboard planetary spacecraft [2–7]. Since this class of space platforms has limited capability for payload due to mass and power constraints, it is instrumental that any additional payload such as an advanced clock be small in volume and mass, and inherently reliable for the expected mission duration that generally average more than 5 years.

To transform the technology of LITS into a spacecraft clock with features mentioned above, several technological advances were developed. To begin with, the size and mass of the LITS as deployed in the DSN were dominated by the four layers of magnetic shielding required to keep the ions from the magnetic perturbation of the outside environment. The design of LITS required that the magnetic shields cover the trap as well as the lamp and the light detection system that is used to optically pump the ions and interrogate their clock transition. These elements include magnetic components that must be kept within the shields to ensure that their residual fields do not change by any interaction with fields external to the clock. This approach was required as the same region in the trap was used to both optically interact with the ions and apply the microwave field that induces the clock transition in the ions.

To reduce the size and weight associated with the magnetic shields that had a diameter of nearly 1 m, a new trap was designed to allow the separation of the optical interaction region from the microwave excitation region. Taking advantage of the electric charge carried by each ion, this new "shuttle trap" has two segments. In the first segment, the ions are produced through collision of electrons emitted from a hot filament with a background of mercury vapor produced by mild heating of an oxide of mercury. The ions were then subjected to the pump light from an RF-excited mercury lamp which produced the optical pumping of the ground hyperfine state ($F = 0$, $^2S_{1/2}$) via the first excited electronic state ($^2P_{1/2}$). After this step which prepared the ions in the $F = 0$ hyperfine sublevel of the ground state, the ions are "shuttled" to a second segment of the trap through the application of a small (a few volts) DC potential. In this region ions are exposed to the microwave radiation (at 40.5 GHz) that induces the $F = 0$ to $F = 1$ clock transition in the ground state before they are shuttled back to the first, optical interrogation, region. Since the ions must be kept isolated from any perturbations only during the interval that they interact with the applied microwave field, a magnetic shielding of the second segment of the trap will be all that is required. As the second segment of the trap is away from the light source and the photon detectors, the size of the shields is reduced by about an order of magnitude.

To further reduce the sensitivity of the ions to external perturbations, a second innovation was introduced to the design of the trap. The conventional design for ion traps used in atomic clocks and frequency standards is based on electrode structures that produce a quadrupole oscillating field. Such a field can be produced with the original hyperbolic electrodes, as well as with the four-rod linear trap. A feature of the quadrupole field is that it contains a node (in the case of the hyperbolic design) or a line of nodes (in the case of the linear trap) where the oscillating electric field applied to the electrodes is zero, and so is the force on the ions. When the ions move away from the node, they experience a ponderomotive force that increases quadratically as they approach any electrode. It is this ponderomotive force that keeps the ions close to the node(s) in the trap. The quadratic increase in the field away from a node, though, results in an increase in the velocity and "heating" on the ions. This effect produces a relatively large second-order Doppler shift that in turn limit the achievable accuracy with trapped ion standards.

At JPL, the microwave interrogation segment of the "shuttle" trap was designed with a multipole electrode configuration. Sixteen rods alternatively excited with the applied oscillating field produce a potential that is essentially zero at the interior of the trap and increases sharply only very close to each electrode. This flat potential allows a much larger region in which the field experienced by the ions is zero, allowing ions to move in a mostly field-free region. Thus the influence of heating and the associated second-order Doppler is greatly reduced.

These innovations have been combined with a design that utilizes small size components, and a sealed vacuum enclosure that is pumped only with

getters to allow a significant reduction in the size of the clock. The current laboratory prototype is essentially smaller than 2 l in volume with a projected mass below 2 kg. The next version being developed will approach the goal of about 1 l in size and 1 kg through improvements in packaging and integration of the electronic circuitry. The projected power requirement is less than 20 W.

The prototype laboratory small clock has already demonstrated a stability performance that breaks into the 10^{-15} region at an averaging interval of about 10,000 s set by the performance of the quartz local oscillator. Similar performance is anticipated for the clock as it is engineered for a 1 kg and 1 l parameters. Such a clock can be used onboard spacecraft to allow one-way navigation. This style of spacecraft navigation, in contrast to the conventional two-way navigation that requires both an uplink and a downlink, does not require an uplink, and will significantly reduce the cost of the SDN operation, while reducing the burden of multiple spacecraft navigation with the same antennas. A modified version of this clock will operate with three different ion species with about a doubling of mass and power. A "triclock" instrument with this geometry can be placed on planetary spacecraft to perform tests of relativity similar to the scheme of the proposed spacetime mission [1].

3 The Quantum Gravity Gradiometer

The development of atom interferometers using laser light pulses to drive stimulated Raman transitions in atoms has provided a sensitive new technique for gravity gradiometry [8]. Unlike gradiometers employing mechanical accelerometers, this approach employs the individual atoms as identical drag-free test masses. The de Broglie wave associated with each atom is then utilized to perform an interferometric measurement of the local acceleration. As in conventional gradiometers, the atom interferometer-based gravity gradiometer employs two accelerometers to allow cancellation, as common-mode noise, of any vibrations of the reference platform. This dual interferometric technique holds great potential for subsurface gravity mapping and monitoring applications, including studies of planetary inner structures and dynamics, changes in ice sheets and ocean currents, changes in underground water storage, and geodesy. The accelerometers can also be used to perform tests of the equivalence principle (EP) with atomic test masses to a sensitivity rivaling proposed measurements with macroscopic test masses in free fall, such as MICROSCOPE [9] and STEP [10]. Toward this end, we are developing at JPL a compact and robust instrument by making extensive use of modular optical components and fiber optics in the laser and optics system, and a highly symmetric geometry in the atomic physics package suitable for microgravity operation.

The current laboratory-based gradiometer consists of two atom interferometers separated by 1.4 m in the vertical direction. The lower interferometer is based on an ultra-high vacuum (UHV) magneto-optic trap (MOT), which is

loaded directly from a two-dimensional MOT-based cesium atom beam source. The two-dimensional MOT generates an atom flux greater than 10^9 atom s^{-1} from a volume of only $4 \times 4 \times 13\,cm^3$, including magnetic coils and optics [11]. The UHV MOT enclosure is a nonmagnetic titanium chamber with high-quality AR-coated windows for optical access. A 250-mm tall vertical tower above the trapping region allows the UHV MOT to operate as an "atom fountain" to obtain long interrogation times in ground-based operation. The same lasers used for trapping and cooling are employed for the state-normalized detection of the launched atoms upon their return. This interferometer geometry is also well suited for microgravity operation, where long-baseline interrogations can be performed simply in the central trap region and under UHV conditions.

The upper interferometer, developed as an early testbed system, is based on a vapor cell MOT. The state selection and normalized detection are performed in a separate detection region, and graphite getters are employed to minimize the background cesium vapor in this region. Due to the different geometry, atoms in the two fountains are launched at different times to operate the interferometers simultaneously.

The modular laser system consists of two frequency-stabilized external-cavity diode lasers as master oscillators and nine injection-locked slave lasers. A phase-locked loop serves the difference frequency between the master lasers to obtain a phase stability better than 1 mrad between 10 Hz and 10 kHz in the Raman lasers. The spectrum of the beatnote between the two Raman frequencies reveals that the central peak contains greater than 99% of the RF power. The master lasers, slave lasers, and frequency-control and beam-splitting modules are interconnected via fiber optics to provide a versatile yet robust laser system. The laser beams for trapping and interferometry are also delivered to the two fountains using fiber optics. The overlapping Raman beams are collimated to 24 mm diameter and aligned vertically through large-diameter (75 mm) windows at the top and bottom of the vacuum chambers for each fountain. The retro-optic for the Raman beams is mounted on a passive vibration isolation platform on the laboratory floor. A schematic of the gradiometer is shown in Fig. 1.

We launch up to 6×10^9 atoms in each atomic fountain at temperatures of 1.8 μK, as measured by stimulated Raman velocimetry. A Doppler-sensitive Raman pulse is applied to select a narrow velocity subgroup so that the remaining atoms are characterized by a one-dimensional temperature of about 100 nK. The atom interferometer is then realized by employing a $\pi/2 - \pi - \pi/2$ stimulated Raman pulse sequence [12]. The difference frequency of the Raman lasers is "chirped" during this sequence to continuously track the Doppler shift of free-falling atoms. By scanning the relative phase of the final $p/2$ pulse, the relative populations of the $F = 3$ and $F = 4$ hyperfine ground states are modulated to produce the interferometer fringes that are observed via laser-induced fluorescence. Interferometer fringes are shown in Fig. 2.

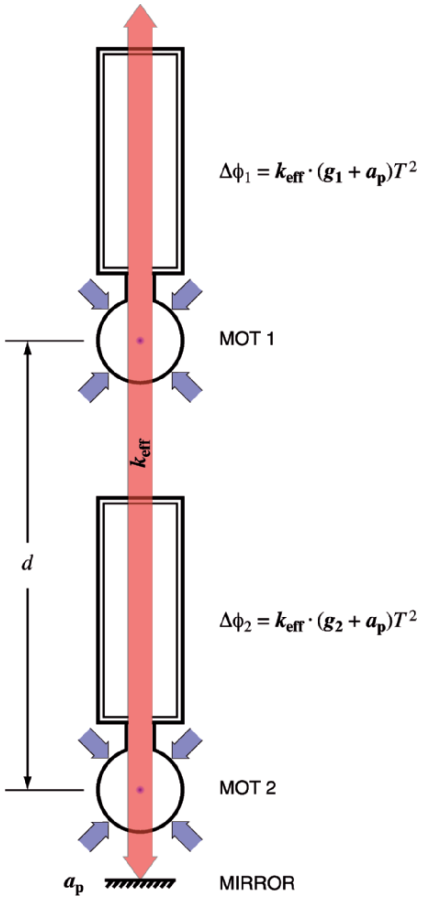

Fig. 1. Illustration of a gravity gradiometer based on dual atom interferometers. The Raman laser along the vertical axis measures the phase shift of atoms in each fountain, so that the gravity gradient along this axis is determined by $\Delta g/\Delta z = (\Delta\phi_1 - \Delta\phi_2)/(k_{\mathrm{eff}}T^2 d)$, and platform vibrations a_p are effectively canceled.

The current instrument has demonstrated a measurement sensitivity of $34\,\mathrm{E\,Hz^{-1/2}}$ ($1\,\mathrm{E} \equiv 10^{-9}\,\mathrm{s^{-2}}$), corresponding to a sensitivity of $5\,\mathrm{E\,Hz^{-1/2}}$ for a 10 m measurement baseline. A second generation instrument is currently being designed with the goal of sensitivity improved by at least an order of magnitude. This second generation instrument will be used for the design and development of a spaceborne instrument for gravity gradiometry in support of geophysical investigations. With relatively small modifications, the same instrument could also be used to test EP at a sensitivity level exceeding all ground-based experiments, and similar to those planned as independent missions.

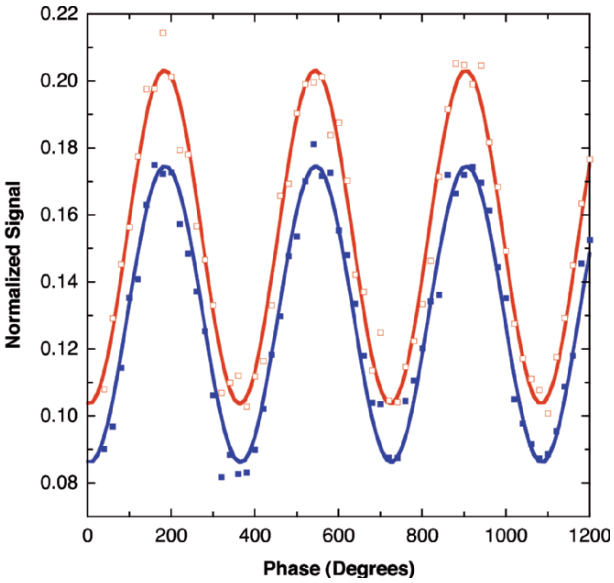

Fig. 2. Simultaneous measurements of atom interferometer fringes in two fountains using a common laser to drive the Raman transitions.

4 Bose–Einstein Condensates for Advanced Atomic-Based Accelerometers

It is widely known in atomic and optical physics community that the Bose–Einstein condensate (BEC) can be used to devise an atom laser producing coherent matter waves. Such a counterpart to the conventional photon-based lasers can be used to improve the sensitivity of matter wave interferometers that are being developed to test fundamental physics, in the same way that photon lasers improve the performance of optical interferometers [13]. Because of this potential to devise vastly improved atom wave interferometers, a program has been underway at JPL to develop a dual-beam atom laser based on spinor condensates [14]. This has led to a recent experimental scheme aimed at the generation of dual atom laser beams, oppositely propagating, with an inherent number correlation between them due to their spin-mixing origin. The novelty of the scheme lies not in the output coupler (simple field gradients that tilt the confining optical potential) but rather in the origin of the outcoupled populations in the dynamics of the coherent spin–spin interaction process. In addition, the presence of a true reservoir and the ability to control both the strength of the output coupler as well as the rate of "pumping" make this a particularly intriguing atom laser scheme.

Our apparatus is built around a single-beam running-wave dipole trap produced by a focused CO_2 laser, which provides at full power a trap depth of approximately 1.6 mK via the DC polarizability of rubidium. We load the

dipole trap from a UHV magneto-optical trap (MOT) which is itself loaded by a cold atomic beam provided by an upstream two-dimensional MOT. The two-dimensional MOT exists in a rubidium vapor cell which is differentially pumped from the adjoining science chamber. All 780 nm trapping light is provided by a unique laser system based on a frequency-doubled 1,560 nm fiber amplifier, described elsewhere. The loading of the dipole trap proceeds according to established technique; we obtain initial populations in the trap of about 2×10^6 rubidium atoms at about 120 μK. The initial trap frequencies (measured via parametric resonance) are approximately 3.2 kHz transversely and 220 Hz longitudinally.

Evaporative cooling proceeds via a programmed rampdown of CO_2 laser intensity. We observed the onset of BEC at critical temperatures near 100 nK, and typically obtain condensates of 10^4 atoms with little or no discernible thermal component. Application of a magnetic field gradient along the weakly trapping axis of the trap during the first few seconds of evaporation preferentially biases out the $m_F = 1$ components, resulting in a BEC solely occupying the field-insensitive $m_F = 0$ projection. Finally, application of a small magnetic field gradient in the vertical direction provides a bias for one or the other polarized components. If this supportive gradient is only on for the first few seconds of evaporation, we obtain polarized condensates of number similar to the other options.

For the observations of the dual-beam laser, we begin with a nominally pure $m_F = 0$ condensate held in a trap whose unperturbed depth is 5 μK and is approximately a factor of 10 weaker due to gravitational tilt. We fix the background field levels at 60 mG as determined by RF spectroscopy. To coherently mix the condensate, we adiabatically compress the trapping field, typically by raising the laser power from 100 to 700 mW over 100 ms, hold the compressed condensate for a variable time, adiabatically expanding, and ballistically expanding while applying the Stern–Gerlach field. We observe that the fraction of atoms evolved into the polarized projections increases with high-density hold time and eventually reaches a static level of 50%. We also observe that the time taken to reach this steady state varies linearly in density, with an offset given by the critical density at which the quadratic Zeeman effect dominates the dynamics.

Slight changes in the offset field, beam tilt, and direction of the extraction gradient affect several variants of the dual-beam atom laser: most commonly, we observe immediate outcoupling and ballistic flight of the $m_F = -1$ component while the $m_F = +1$ component first propagates in the opposite direction (as expected), then reverses its motion, passes through the parent $m_F = 0$ condensate, and escapes along a different trajectory (see Figs. 3 and 4). We also observe the more intuitive case of both polarized components escaping into ballistic flight from opposite ends of the cigar-shaped trap.

Future work will explore the nature of correlations and entanglement in these beams, the possibility of spin-independent outcoupling, and also explore the possibilities of improving this process into the quasicontinuous regime.

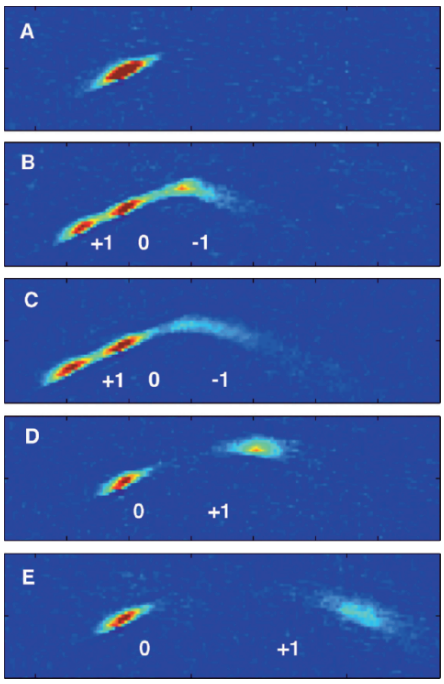

Fig. 3. A typical outcoupling run of the spinor dynamics-driven dual-beam atom laser. (**a**) 0 ms: the full condensate, in situ. (**b**) +20 ms: immediately after outcoupling. The $m_F = -1$ component immediately passes beyond the reach of the dipole trap and experiences ballistic flight and mean-field expansion. The $m_F = +1$ component remains confined in an effective guide and travels in the opposite direction. (**c**) +25 ms: the $m_F = -1$ beam continues to propagate while the $m_F = +1$ beam is turned around and returned toward the origin. (**d**) +45 ms: the $m_F = +1$ beam now falls freely and experiences mean-field expansion, like the $m_F = -1$ component before it. Note a slightly different path than $m_F = -1$. (**e**) +50 ms: continued $m_F = +1$ propagation; note the $m_F = -1$ component has traveled out of the field of view by this point. Images are 1–0.25 mm; gravity is directed toward the *lower right* and the trapping laser is directed toward the *upper right*.

Finally, it should be possible to implement a number measurement on one outcoupled component, rendering the untouched component into a known Fock state and thus ideal for Heisenberg-limited phase measurements. The scheme of the dual-beam atom laser can be tailored for applications with atom interferometry with a sensitivity beyond what is achieved with conventional laser cooled clouds.

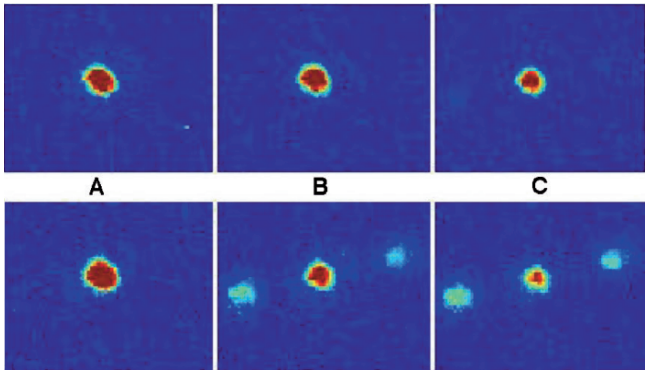

Fig. 4. The effect of adiabatic compression on the spin-mixing process; the *top row* shows condensates held for equivalent durations without compression. (**a**) 100 ms of hold time at 700 mW, (**b**) 400 ms of hold time, (**c**) 1.2 s of hold time. The slightly fewer overall number in (**c**) is due to condensate lifetime. The ballistic expansion time for all images is 17.5 ms. Images are 1–0.8 mm.

5 Summary

In this chapter we have presented a summary of technology development efforts at JPL aimed at demonstration of instruments for use in NASA missions in support of navigation and earth and planetary exploration. By designing these instruments based on approaches that support fundamental physics investigation, we hope to gain access to space platforms that are otherwise unavailable to the fundamental physics community. This strategy is aimed at keeping the prospects of laboratory style experimental tests of physics in space alive in an era when support for such investigations has been largely abandoned in favor of observational experiments, and manned flights.

The research described in this chapter was carried out at the Jet Propulsion Laboratory, California Institute of Technology, under a contract with the National Aeronautics and Space Administration.

References

1. L. Maleki and J. Prestage: Search for New Physics with Atomic Clocks Astrophysics, Clocks and Fundamental Constants Eds. S G Karshenboim and E Peik (Berlin:Springer, 2004).
2. J.D. Prestage, G.J. Dick, and L. Maleki: J. Appl. Phys. **66**, 1013 (1989).
3. J.D. Prestage, R.L. Tjoelker, L. Maleki: Phys. Rev. Lett., **74**, 3511 (1995).
4. J.D. Prestage, R.L. Tjoelker, L. Maleki: Proc. 2000 IEEE Freq. Control Symp., pp. 459–462 (2000).
5. J.D. Prestage, R.L. Tjoelker, L. Maleki: Topics Appl. Phys. **79**, 195–211, Frequency Measurement and Control, ed. A.N. Luiten (2001).

6. J.D. Prestage, S. Chung, E. Burt, L. Maleki, and R.L. Tjoelker: Proc. 2002 IEEE Freq. Control Symp., pp. 706–710 (2000).
7. R.L. Tjoelker, J.D. Prestage, P.K. Koppang, and T.B. Swanson: Proc. 2003 IEEE Freq. Control Symp., pp. 1066–1072 (2003).
8. J.M. McGuirk, G. Foster, J.B. Fixler, M.J. Snadden, and M.A. Kasevich: Phys. Rev. A **65**, 033608 (2002).
9. P. Touboul, Space Accelerometers: Present Status. In C. Lämmerzahl, C.W.F. Everitt and F.W. Hehl (eds.). *Gyros, Clocks, Interferometers ...: Testing Relativistic Gravity in Space*. (Springer, Berlin 2001).
10. N. Lockerbie, J.C. Mester, R. Torii, S. Vitale, and P. Worden. STEP: A status Report. In C. Lämmerzahl, C.W.F. Everitt and F.W. Hehl (eds.). *Gyros, Clocks, Interferometers ...: Testing Relativistic Gravity in Space*. (Springer, Berlin 2001).
11. J. Ramirez-Serrano, N. Yu, J.M. Kohel, J.R. Kellogg, and L. Maleki: Opt. Lett. **6**, 682–684 (2006).
12. M. Kasevich and S. Chu: Phys. Rev. Lett. **67**, 181 (1991).
13. N. Lundblad, R.J. Thompson, D. Aveline, and L. Maleki: Submitted to PRA (2006).
14. D.M. Stamper-Kurn, et al., Phys. Rev. Lett. **83**, 661 (1999).